

A New EMI Filter Selection Method and a Comparison with the Existing Radiation-based Method

UDK 621.372.54
 IFAC 5.8.0

Original scientific paper

This article describes a new method for the selection of an appropriate signal line Electromagnetic Interference (EMI) filter. It describes an EMI filter selection method based on the signal's FFT measurement. This selection has proved to be efficient also for quick engineer use. We optimize the EMI filter for each single line separately. The method described in this article involving a Central Processor Unit (CPU) module demonstrates the comparison between new FFT-based selection method and the existent radiation-based one.

Key words: EMC, EMI filter, critical line length, critical frequency

1 INTRODUCTION

There are two EMI filter selection methods. The first one is based on radiation measurements. The radiation of the entire device is measured, which provides a discrete frequency component with the maximum amplitude. The EMI filter with maximum insertion loss close to this discrete frequency component is selected. The resulting filters have the same frequency characteristics within the entire device. The second method has been developed and tested in the EMC Laboratory of the ISKRAEMECO d.d. Company. It is based on the FFT measurements on a single signal line.

The main advantage of the new method is that a filter is selected for each single line separately. This gives better results in terms of EMC problem solving than the existent radiation-based method. It is very important that the new method is suitable for quick engineer use. The comparison between this new EMI filter selection method and the existent radiation-based method is showed in chapter 6.

2 CRITICAL LINE LENGTH

An expression »critical line length« is known from high speed transmission-line theory [2]. What is a long transmission-line? That depends on the transmitted frequencies. A frequency spectrum of a digital periodic signal (a trapezoidally shaped wave) is presented in Figure 1.

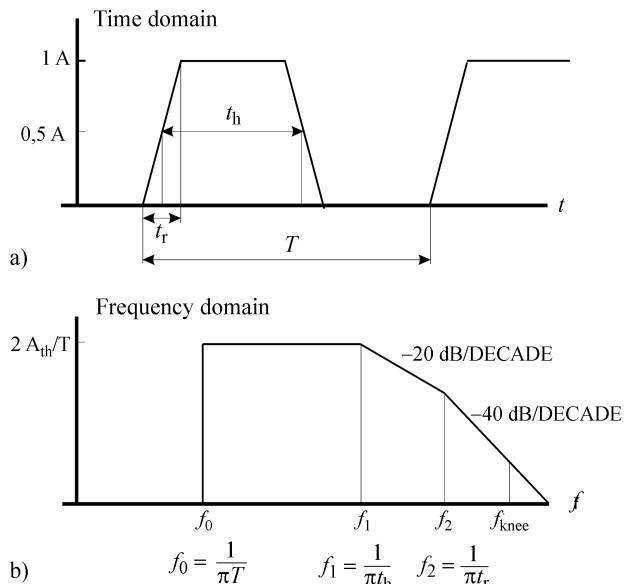


Fig. 1 Spectrum of digital periodic signal

This signal can be described as series spectral components

$$f(t) = \frac{A_0}{2} + \sum_{n=1}^{\infty} [A_n \cos(n\omega_0 t) + B_n \sin(n\omega_0 t)]. \quad (1)$$

The coefficients A_0 , A_n in B_n are found as

$$\omega_0 = \frac{2\pi}{T}, \quad (2)$$

$$A_0 = \frac{2}{T} \int_{t_0}^{t_0+T} f(t) dt, \quad (3)$$

$$A_n = \frac{2}{T} \int_{t_0}^{t_0+T} f(t) \cos(n\omega_0 t) dt, \quad (4)$$

$$B_n = \frac{2}{T} \int_{t_0}^{t_0+T} f(t) \sin(n\omega_0 t) dt. \quad (5)$$

Where are:

ω_0 – basic angular frequency,

T – period of the signal,

t_0 – time in the moment of observation.

For the trapezoidal signal shown on Figure 1a, we find

$$A_n = 2A \frac{t_h}{T} \frac{\sin\left(n\pi \frac{t_h}{T}\right)}{n\pi \frac{t_h}{T}} \cdot \frac{\sin\left(n\pi \frac{t_r}{T}\right)}{n\pi \frac{t_r}{T}}, \quad (6)$$

where:

A – amplitude – point to point,

t_h – pulse width

t_r – rise time,

t_f – fall time,

T – period of the signal,

n – harmonic number.

This spectrum consists of discrete frequency components $f_n = nf_T$, where $f_T = 1/T$. When we draw asymptotes to this spectrum, we find a horizontal line up to the first corner frequency (Figure 1b)

$$f_1 = \frac{1}{\pi t_h}, \quad (7)$$

and from there a descending line at a rate of decrease of 20 dB/dec up to the second corner frequency (Figure 1b)

$$f_2 = \frac{1}{\pi t_r}. \quad (8)$$

For higher frequencies, the rate of decrease is 40 dB/dec (Figure 1b).

$$f_{\text{knee}} = \frac{1}{2t_r}. \quad (9)$$

Frequency f_{knee} is a practical maximum which is about 1.5 times f_2 .

The critical line length is determined by the frequency f_{knee} . It is well known that electromagnetic

emission increases with frequency until a half the wavelength of the signal exactly fits the length of the trace.

$$f_{\text{knee}} = \frac{1}{2t_r}, \text{ Hz, signal property} \quad (10)$$

$$\frac{\lambda_{\text{knee}}}{2} = \text{length of the line, m, line property.} \quad (11)$$

The propagation on the line is

$$v_{\text{prop}} = \frac{l_{\max}}{t_{\text{pd}}} = \frac{1}{\sqrt{\mu\epsilon}}, \text{ m/s.} \quad (12)$$

t_{pd} is the propagation delay. The wavelength in equation (11), can be written as

$$\lambda_{\text{knee}} = \frac{v_{\text{prop}}}{f_{\text{knee}}}, \text{ m,} \quad (13)$$

with equations (10) and (12) we find a critical line length l_{\max}

$$l_{\max} = \frac{\lambda_{\text{knee}}}{2} = \frac{\frac{v_{\text{prop}}}{f_{\text{knee}}}}{2} = \frac{1}{\sqrt{\mu\epsilon}} t_r, \text{ m.} \quad (14)$$

At the critical line length the rise-time t_r exactly matches the two-way propagation delay time t_{pd} (source-load-source). This means that the transient phenomenon formed by the low-to-high signal transition precisely fits the line length. For that reason, this distance is called the length of the rising edge [2]. We must stress that the critical line length l_{\max} means two-way propagation delay (source-load-source).

To simplify equation (14), the real value of propagation delay for FR-4 – currently the most commonly used material in the production of printed circuit boards (PCBs) – is used. With equations (15) and (16) the maximum electrical line length before the required line termination is determined. The calculations below are used for the dielectric constant of FR-4 material ($\epsilon_r = 4.6$). The latter varies with signal frequency within the material. Most engineers generally assume ϵ_r to be in the range of 4.5 to 4.7. These are the values that are published in various technical references [3].

$$l_{\max} = 9 \cdot t_r, (T_r - \text{in ns}) \\ (\text{for microstrip topology - in cm}), \quad (15)$$

$$l_{\max} = 7 \cdot t_r, (T_r - \text{in ns}) \\ (\text{for stripline topology - in cm}). \quad (16)$$

A line length equal to or longer than the critical length definitively behaves as a transmission line. Characteristic impedance, delay and reflections should not be ignored. At the same time, it also behaves as an efficient antenna and is reflected in considerable electromagnetic radiation and susceptibility problem. Corrupted signals are usually rich on higher frequency components.

3 TYPICAL FREQUENCY – OBSERVED AS EMI

Typical frequency – observed as EMI – depends upon used logic elements and microcontroller. More precisely, it depends upon the rise time of the signals transmitted by these elements (17). Special attention should therefore be paid to the selection of appropriate logic elements and microcontroller. If, for instance, a faster High-speed CMOS with TTL inputs (HCT) instead of a slower Low-power Schottky transistor-transistor logic (LS-TTL) is used, the electromagnetic emission can increase up to three times. As might be expected, a discrete frequency component at typical frequency starts to emit electromagnetic disturbances at a certain line length at which it becomes an efficient antenna [3].

$$f_{\max} = \frac{10}{\pi t_r}. \quad (17)$$

These typical frequencies – observed as EMI are very important when designing an electronic circuit.

To check the accuracy of the equation (17), the amplitude of the discrete frequency component at the typical frequency – observed as EMI – was measured [9]. The measurement equipment proved to be inadequate. We measured with four channels oscilloscope Tektronix TDS744A with maximum digitizing rate 2 GS/s and analog bandwidth 500 MHz. This was too low for 74 Advanced CMOS (74AC) logic with a typical frequency of 1.6 GHz. For that reason the 74HC logic with a typical frequency of 270 MHz was chosen.

Figure 2 shows the output signal from 74HC245 logic circuit. The frequency spectrum rises again at frequencies in the range 220–300 MHz. The peak with the amplitude of 28.64 dB is located at the typical frequency of 265.258 MHz.

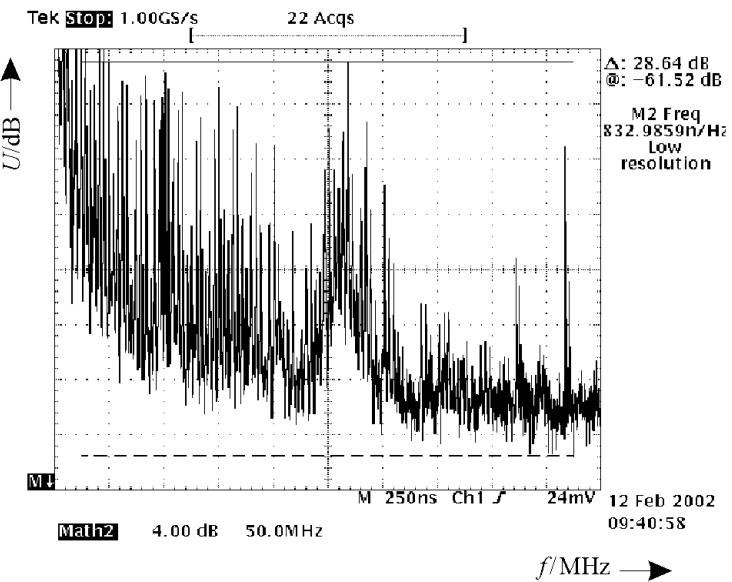


Fig. 2 FFT of an output signal from 74HC245 logic circuit

We measured rise time t_r of the signal and we got 12 ns. Then we calculated the typical frequency – observed as EMI from equation (17). We obtained 265.258 MHz. We obtained the same result (18) as with the measurement.

$$f_{\max} = \frac{10}{\pi t_r} = \frac{10}{\pi \cdot 12 \text{ ns}} = 265.258 \text{ MHz}. \quad (18)$$

The calculation of the typical frequency – observed as EMI – is relatively simple. Its accuracy was also confirmed by the measurement.

4 SELECTION OF AN APPROPRIATE EMI FILTER STRUCTURE

EMI filter insertion losses are handled at 50Ω input and output impedance [5]. Normally, such

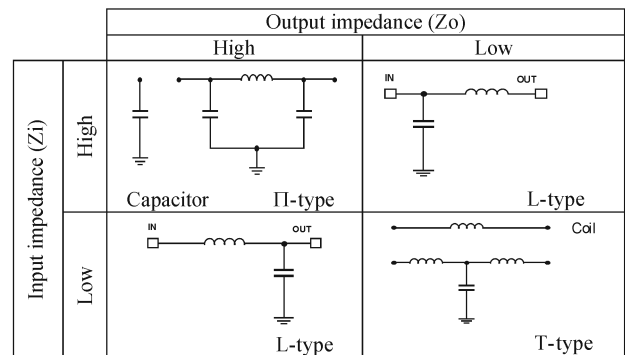


Fig. 3 Selection of an appropriate EMI filter structure

impedance does not exist in real electronic circuits. It is a well-known fact that EMI filter performance strongly depends on the input and output impedance. This is the impedance of the surrounding electronic circuit. Some general rules for selection of an appropriate EMI filter structure should be considered (Figure 3) [6]. The fact is that capacitors are best used in high impedance circuits, whereas coils are best used in low impedance circuits. The reason lies in component characteristics at high frequencies [8]. A suitable EMI filter structure can be selected using the table in Figure 3.

5 SUITABLE EMI FILTER SELECTION

The procedure for a proper EMI filter selection consists of the following steps:

- Define a signal rise time t_r – from the used logic elements;
- Calculation of the typical frequency – observed as EMI;
- Selection of a suitable EMI filter family with regard to the application requirements;
- Selection of an EMI filter from the family which has the maximum insertion loss at the approximate typical frequency.

The need for the use of EMI filters depends upon the critical line length which has been verified in practice [7]. If a two-way line length is shorter than the previously calculated l_{max} (critical line length) and if there are no via connections on the line, the use of an EMI filter is not necessary.

A procedure of EMI filter selection method described above is presented on Figure 4.

6 EXPERIMENTAL WORK

Some tests were made on the CPU module. In the first stage, we did not consider EMC developing rules. Two layers printed circuit board was used. The density of lines was high. Radiated emission was measured. The result of this measurement is presented on Figure 5. The uninterrupted horizontal line illustrates maximal allowed radiated emission according to the standard EN 55022 - B.

The second stage was followed. All EMC radiation emission reduction technics were considered in this stage. Eight layers printed circuit board was used now. We did not use EMI filters yet. Radiated emission was measured once again. The result of this measurement is presented on Figure 6.

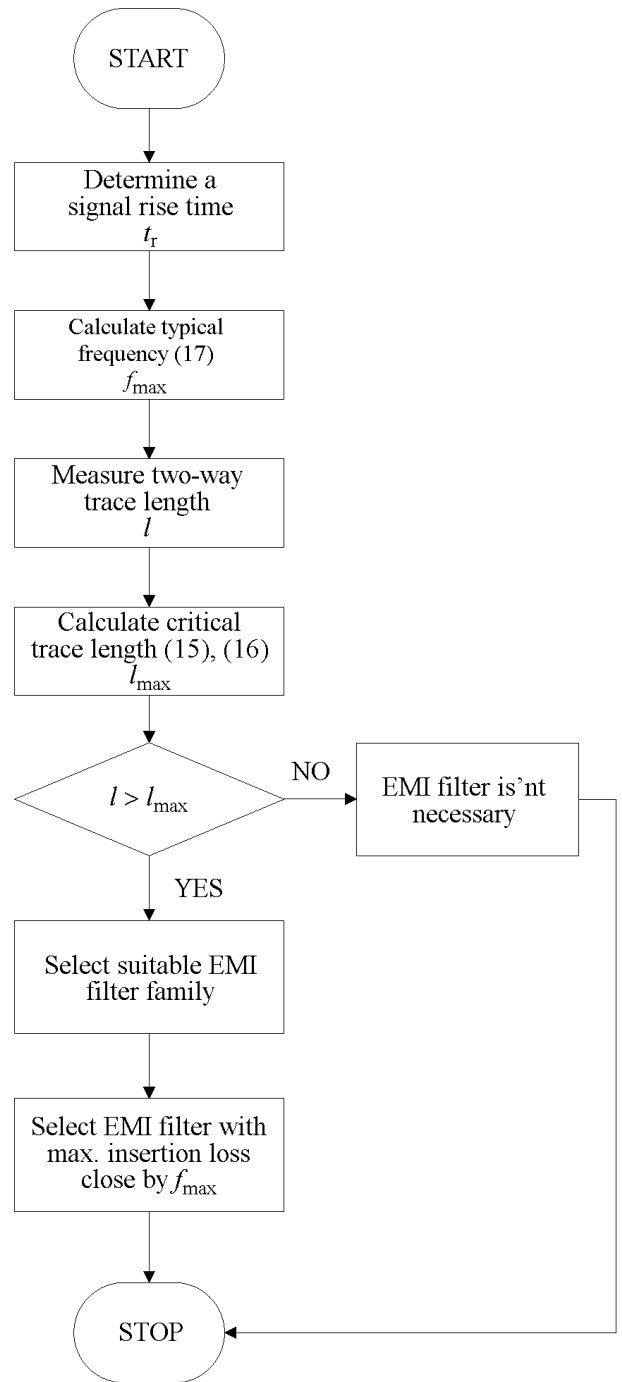


Fig. 4 A suitable EMI filter selection method

In the third stage, CPU module was equipped with EMI filters. Filters were selected with the radiation-based method and the radiated emission was measured. It was below the allowed limit but still rather high (Figure 7).

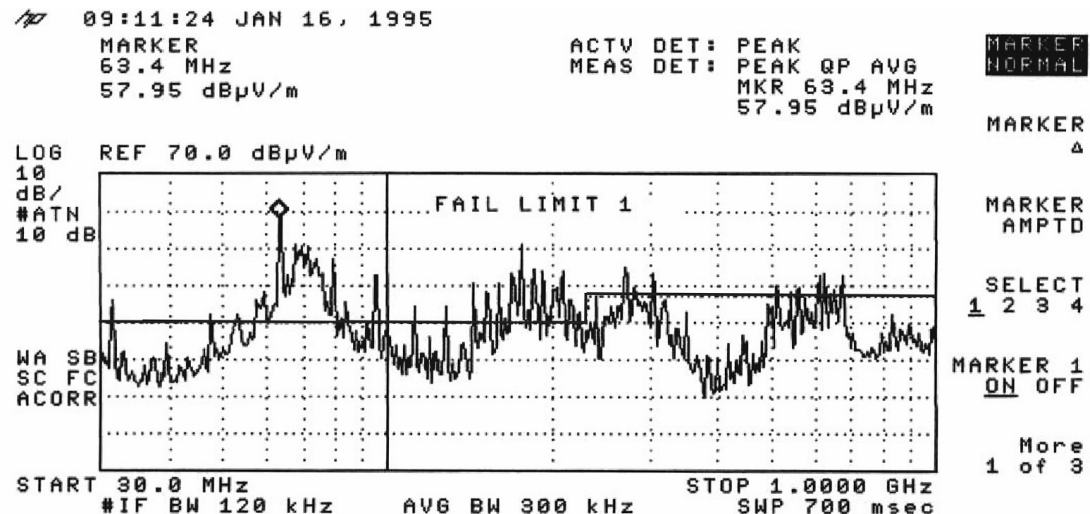


Fig. 5 Radiated emission (two layers printed circuit board)

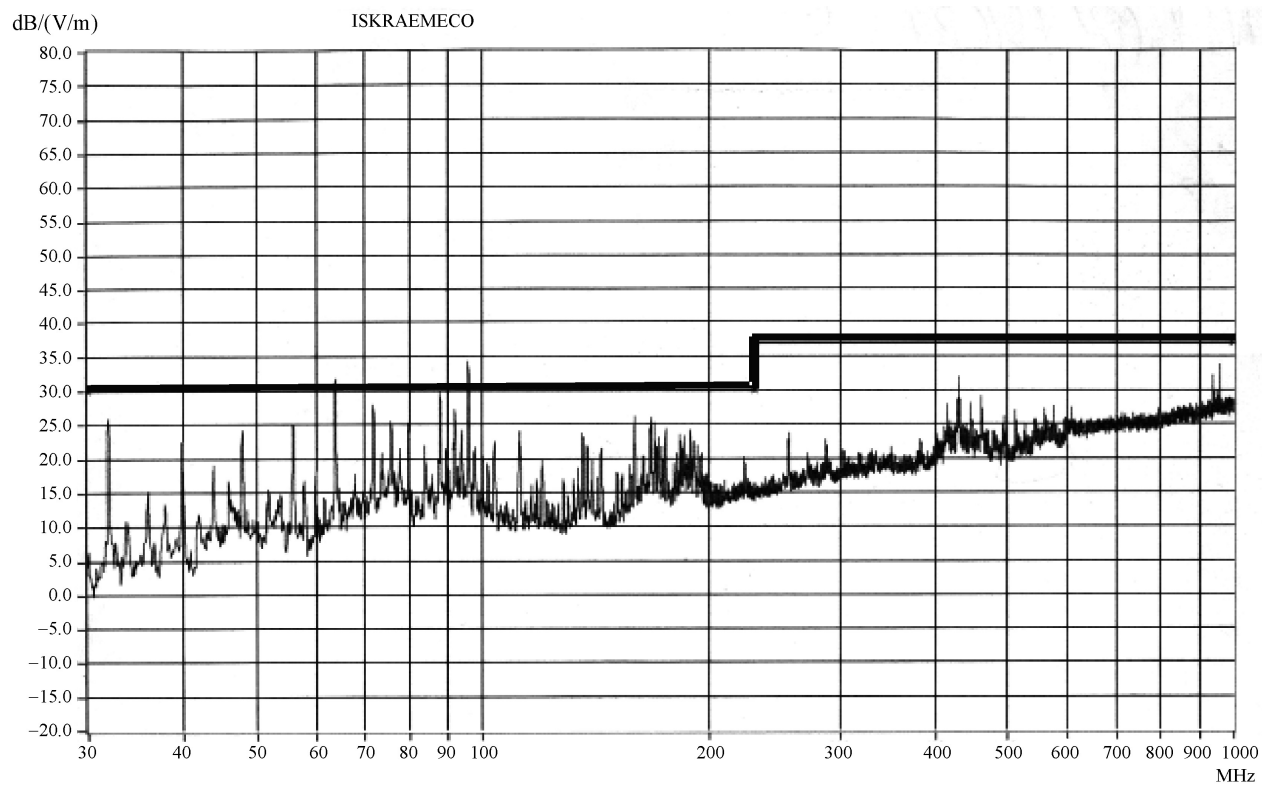


Fig. 6 Radiated emission (eight layers printed circuit board)

Finally, EMI filters selected according to the new method were installed in the same CPU module. As expected, the radiation level was significantly lower (Figure 8).

The tests performed on the CPU module clearly demonstrate that the proposed FFT-based EMI filter selection method is better than the radiation-based one.

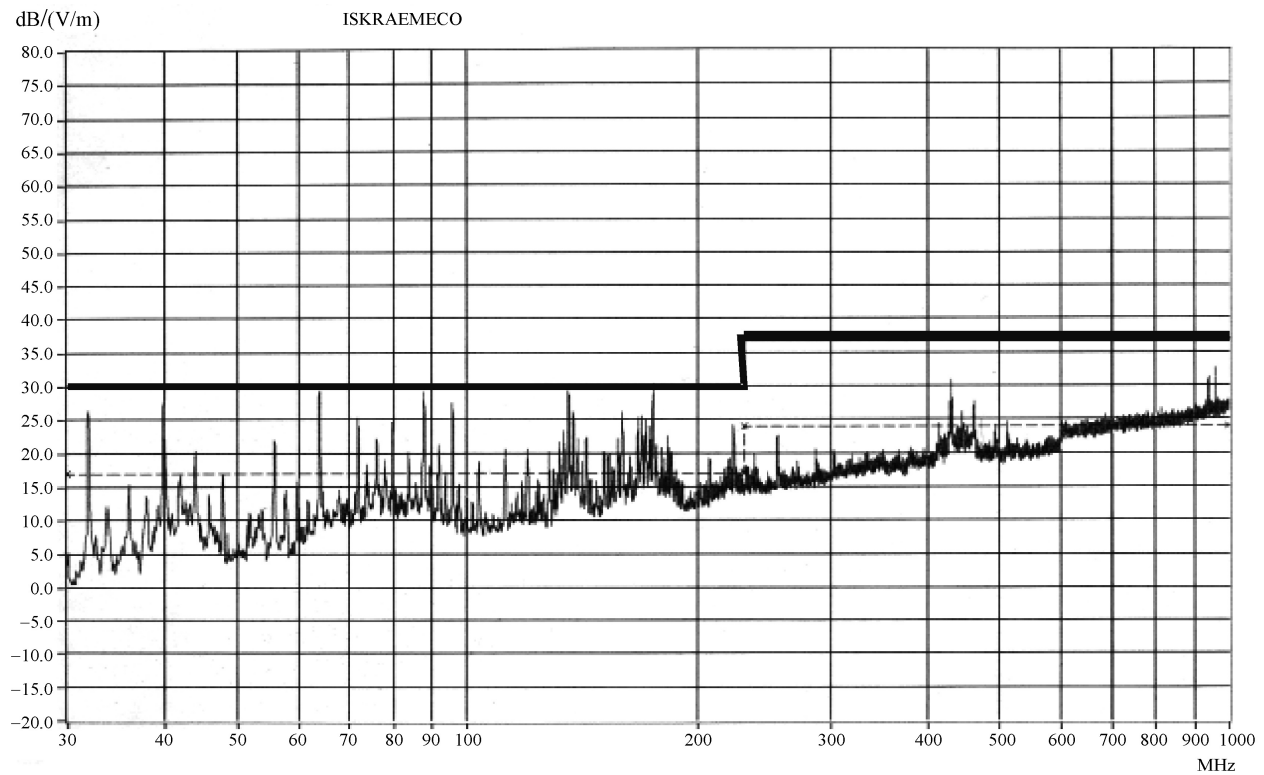


Fig. 7 Radiated emission (EMI filters, radiation-based method)

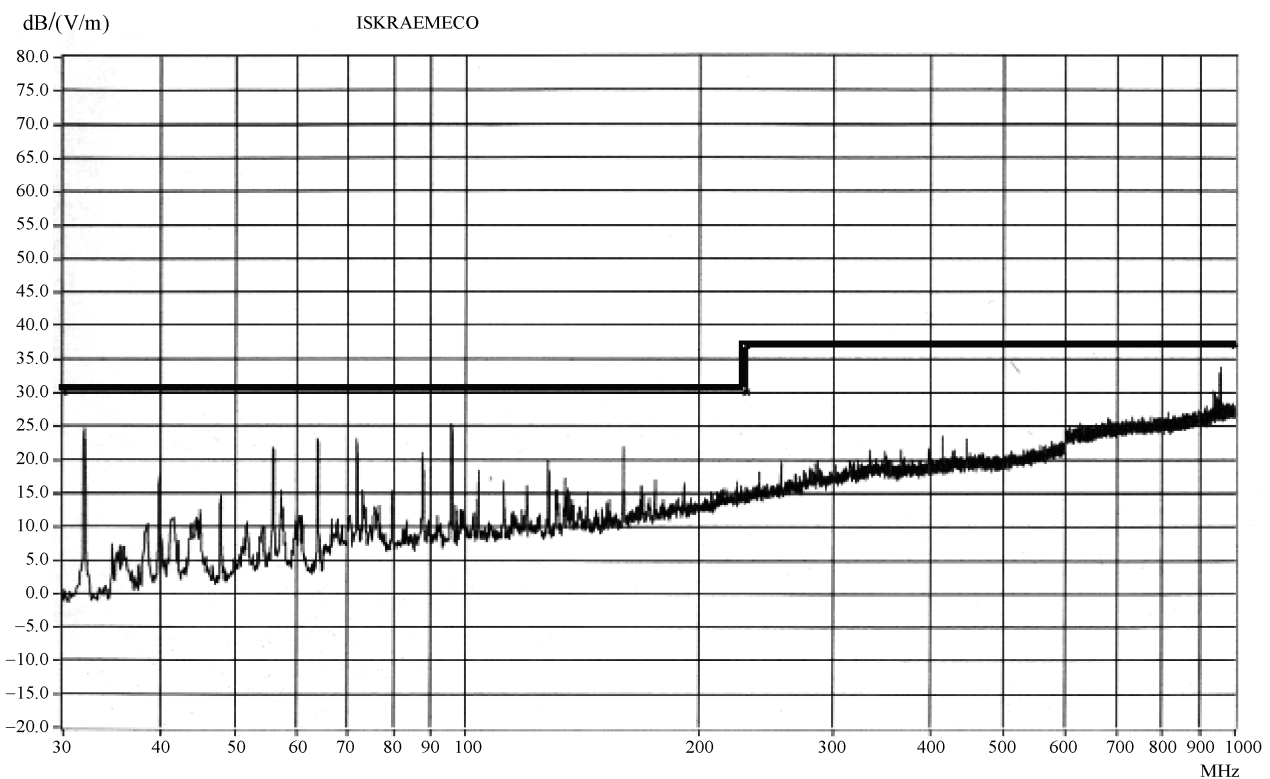


Fig. 8 Radiated emission (EMI filters, new method)

7 CONCLUSION

Generally, a selection of suitable EMI filters is very important for designing. We can not always solved EMC emission problems without EMI filters. The tests performed on the CPU module clearly demonstrate that the proposed FFT-based EMI filter selection method is better than the radiation-based one.

The main advantage of this new method is that it suitable for quick engineer use and that solves EMC emission problems separately for each single signal line, which is why we believe it produces better results.

REFERENCES

- [1] D. Campbell, H. Kreidl, **Solving EMC Issues**. Motorola, Workshop 36, EMV'03, pp. 116, Augsburg, 2003.
- [2] F. J. K. Buesink, **Thomson – CSF Signaal, Henglo, NL, High Speed Digital Design Topics for Printed**

Circuit Boards. Workshop 24, EMV'01, pp.11–12, Augsburg, 2001.

- [3] M. I. Montrose, **EMC and the Printed Circuit Board: Design, Theory, and Layout Made Simple**. First edition, IEEE Press Editorial Board, vols 1, 3, 6, 7, pp. 1–212, New York, 1999.
- [4] S. Kazama, S. Shinohara, R. Sato, **Evaluation of Methods of Measuring Digital IC Terminal Output**. EMC Research Laboratories Co., Ltd., pp. 329–334, Sendai, Japan, 2000.
- [5] V. Đ. Desnica, L. D. Živanov, O. S. Aleksić, M. D. Luković, M. D. Nimirhiter, **Comparative Characteristics of Thick-Film Integrated LC Filters**. IEEE transactions on instrumentation and measurement, vol. 51, no. 4, pp. 570–576, august 2002.
- [6] ..., muRata, **Noise Suppression by EMI Filtering: Basics of EMI Filters**. No. TE04EA-1, pp. 1–4, 1998.
- [7] M. Šegula, M. Podberšič, **Reševanje EMC problematike**. ISKRAEMECO, d.d., pp. 1–56, Kranj, 2002.
- [8] D. Anderson, L. Smith, J. Gruszynski, **S-Parameter Techniques for Faster, More Accurate Network Design**. Hewlett-Packard Company, pp. 4–13, USA, 1996–1997.

Novi postupak odabira EMI filtra i usporedba s postojećim postupkom temeljenim na radijaciji.
Ovaj članak opisuje novi postupak za odabir odgovarajućeg elektromagnetsko-interferentnog (EMI) filtra linije signala. Opisana je metoda odabira EMI filtra temeljena na mjerenu spektra signala (FFT). Ovakav odabir se, također, pokazao kao efikasan za brzu inženjersku primjenu. Optimizira se EMI filter posebno za svaku liniju signala. Metoda opisana u ovom članku koristi CPU modul i prikazuje usporedbu novog postupka odabira temeljenog na FFT-u i postojećeg postupka temeljenog na radijaciji.

Ključne riječi: EMC, EMI filter, kritična duljina linije, kritična frekvencija

AUTHORS' ADDRESSES

- dr. Marko Podberšič**
Ministry of Defence, Administration for Civil Protection and Disaster Relief
Vojkova cesta 61, 1.000 Ljubljana, Slovenia.
- prof. dr. Vojko Matko**
University of Maribor, Faculty of Electrical Engineering and Computer Science
Smetanova ulica 17, 2.000 Maribor, Slovenia

Received: 2007-05-21